QFT Report

Mohammad Odeh – Dec. 20th, 2023

This report serves to describe the procedure taken in attempting to design a set of robust controllers for the FOWT MIMO system using the QFT framework. It is an update on the previously report submitted on Nov. 24th, 2023. In this report, a single approach was taken; Independent SISO controller design, which is discussed in detail in Dr. Mario Garcia-Sanz book "Robust Control Engineering: Practical QFT Solutions (2017)".

Model Setup and Plant Generation

Before we can begin designing the controller us the QFT framework, we first need to generate a model of the plant along with the uncertainties associated with it. For this purpose, the FOCAL turbine model from within the CRAFTS platform was used. A specific model used for the QFT design was derived from the original, basic FOCAL turbine that was tested and verified thoroughly throughout campaigns 1 and 2 of phase I of the ARPA-e project.

This model was modified to accommodate for the desired I/O combination to be used in the QFT plant generation. For the inputs, 4 channels were selected: CPC and IPC 1-3. For the outputs, 4 channels were selected: RotSpd and BRBM 1-3. For the sake of simplicity, the generator torque (defined as $P_{ref}/RotSpd$) along with wind source were embedded within the model that is to be linearized. A screenshot of the model used can be found below.

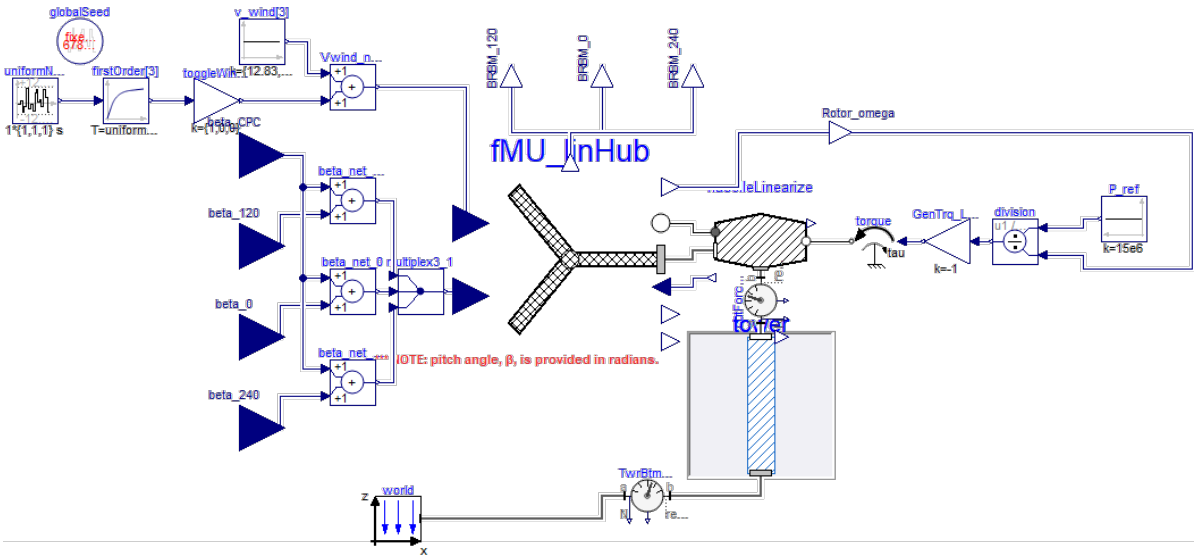

Figure 1: Linearized model

The linearized model wind source was fixed at $12.83\ m/s$, maintaining the turbine operation strictly in regime 3. Similarly, the rotor speed (RotSpd) was initially set at $7.56\ rpm$ to ascertain that the turbine is operating in regime 3 at startup of the simulation.

To linearize the model, the Dymola generated FMU is imported into Simulink using the FMIKit developed and maintained by CATIA (Dassault Systèmes). With the FMU imported into Simulink, the "Time-Based Linearization" block was used to linearize the system after steady-state operation of the turbine was reached.

For the plant uncertainty, the azimuth angle (Ψ) was chosen as the parameter to be varied, starting from $0°$ through $360°$, stepping in $15°$ increments such that $\Psi \in [0, 15, 30, \dots, 345, 360)$, yielding 24 distinct plants.

Independent 4x4 MIMO Model (Chapter 8, Example 8.1, Page 186 – 192)

In this approach, we deal with the MIMO system as a set of 4x4 independent SISO systems. This facilitates the design of the controller by sacrificing performance and allowing interactions across all channels due to coupling. A practical approach to finding I/O pairing is by using the RGA matrix defined as $\Lambda = P_0 \otimes (P_0^{-1})^T$, where P_0 is the $n \times n$ nominal plant at steady-state $(\omega = 0)$ which is chosen to be the plant at $\Psi = 0°$ and the operator $\otimes$ denotes element-wise multiplication (also known as Hadamard or Schur product). Ideally, the I/O pairing corresponds to the elements of the RGA matrix closest to one.

```
%   Example:
%                                          _    u1      u2      u3    _
%                                         |  0.3180  0.0195  0.6630  | y1
%       Λ_0 = P(s=0) .* (P(s=0)^-1)^T = |  0.6820  0.0091  0.3090  | y2
%                                         |_    0    0.9710  0.0287 _| y3
%
%   According to RGA matrix, pairing is:
%       ( u1, y2 ) --- ( u2, y3 ) --- ( u3, y1 )
%
```

However, for the sake of simplicity and due to symmetry, the I/O channels IPC 1-3 were assigned to BRBM 1-3 and CPC to RotSpd, respectively. This pairing allowed for the successful generation of 4 controllers, the first corresponding to CPC – RotSpd channel and the remaining corresponding to IPC 1-3 – BRBM 1-3 channel. Note that the average of all generated plants was used as the nominal plant, P_0.

The transfer functions (TFs) generated have the following form.

$$\frac{RotSpd}{CPC} = \frac{-0.35s\,(s+627)(s+65.23)(s^2+692.2s\ +\ 1.59\times10^5)^2}{(s+0.04016)\,(s+5.676\times10^{-5})\,(s^2+\ 692.2s\ +\ 1.59\times10^5)^3}$$

$$\frac{BRBM_i}{IPC_i} = \frac{-3.82\times10^8\,(s+9079)\,(s+17.59)\,(s+0.046)\,(s+4.73\times10^{-5})}{(s+0.04016)\,(s+5.676\times10^{-5})\,(s^2+\ 692.2s\ +\ 1.59\times10^5)}\ ,\quad i=1,2,3$$

The controllers that were designed have the form of

$$g_{11}(s) = \frac{-0.031008\,(s+321.1)\,(s+0.3649)}{(s+0.7792)\,(s+0.7692)}$$

$$g_{jj}(s) = \frac{-1.9698\times10^{-8}}{(s+13.66)\,(s+0.01361)}\ ,\qquad jj=2,3,4$$

where the controller $g_{11}(s)$ corresponds to the CPC – RotSpd channel, and the controllers $g_{jj}(s)$ corresponds to the IPC 1-3 – BRBM 1-3 channels. Furthermore, the controller $g_{11}(s)$ was saturated at $\beta_{CPC} \in [0,\ \pi/2]\ rad/s$ while the controllers $g_{jj}(s)$ were limited to operate in the range of $\beta_{IPC} \in [-0.035,\ 0.035]\ rad/s$. An illustration of the simulated model can be found in the image below.

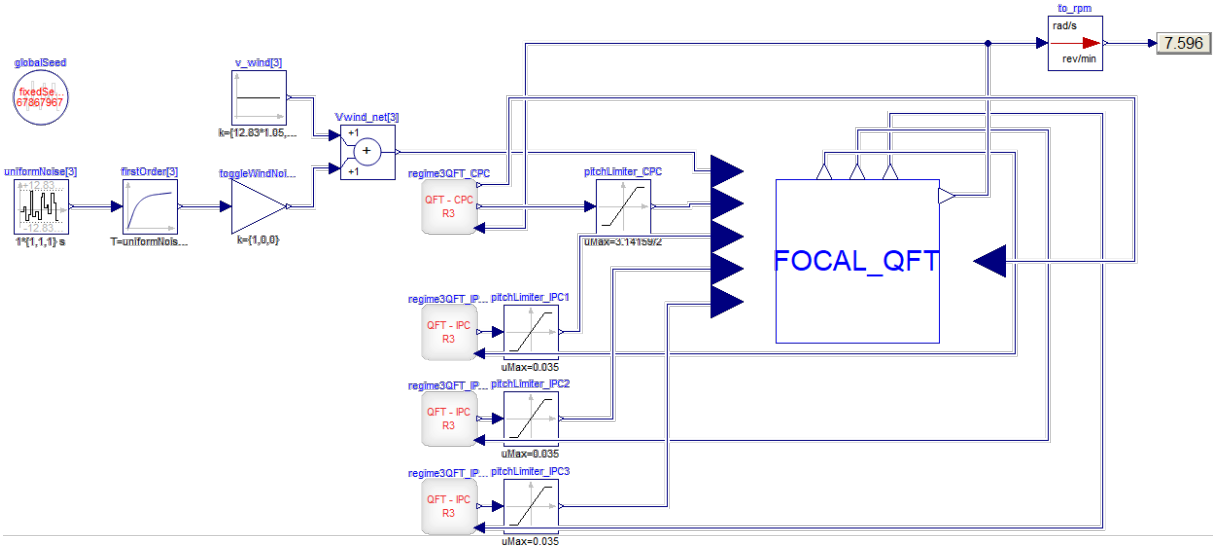

Figure 2: Simulated model

The generated QFT bounds are presented below for P_{0_11} and P_{0_22} since P_{0_33} and P_{0_44} look exactly similar.

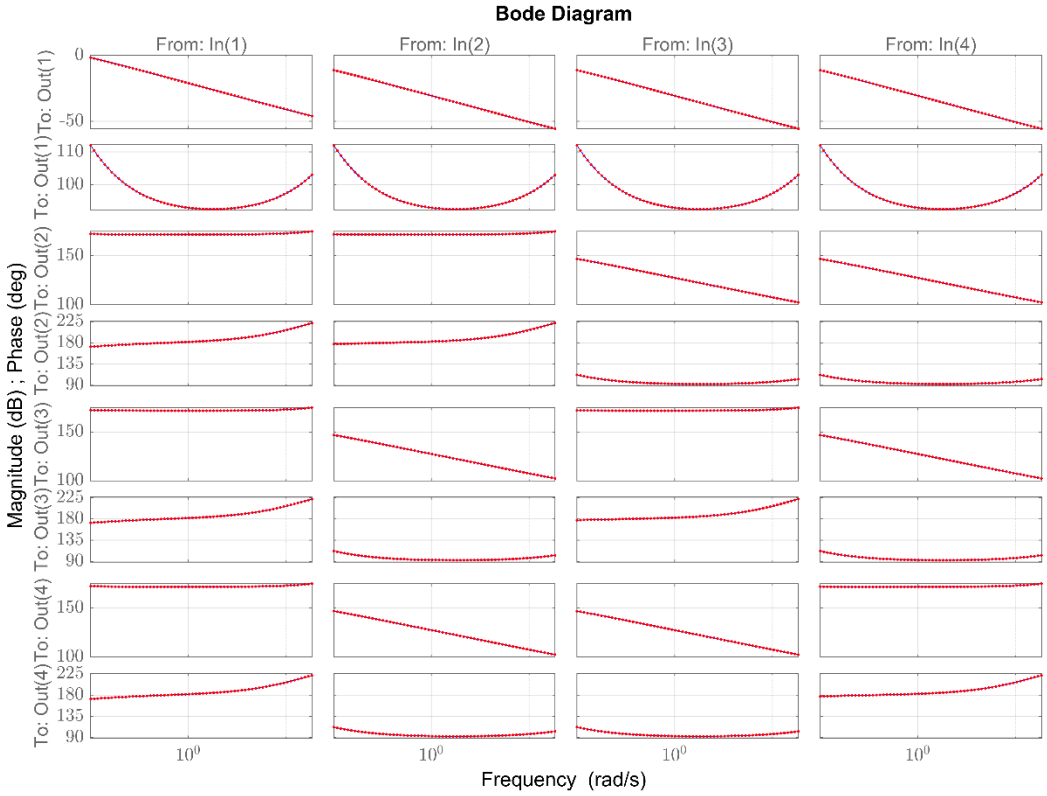

Figure 3: Bode Plot

From the Bode plot, we can see that the IPC/BRBM entries have a lot more weight and influence, indicating that a proper design of the IPC channel will have a dominant role on the performance of the controlled turbine. This has been validated by implementing the designed controllers set and then disabling the IPC channel while maintaining the CPC channel active. While the turbine tracked the reference target for RotSpd, it had higher then expected deviation from the rated speed.

The generated plant templates for the diagonal elements are also presented below,

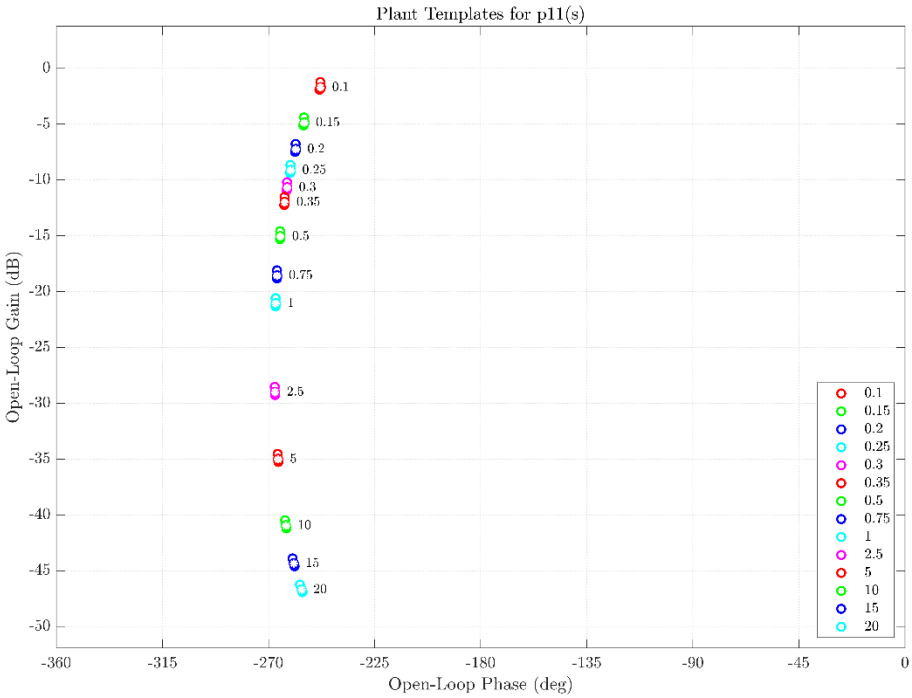

Figure 4: Plant template for P_{11}

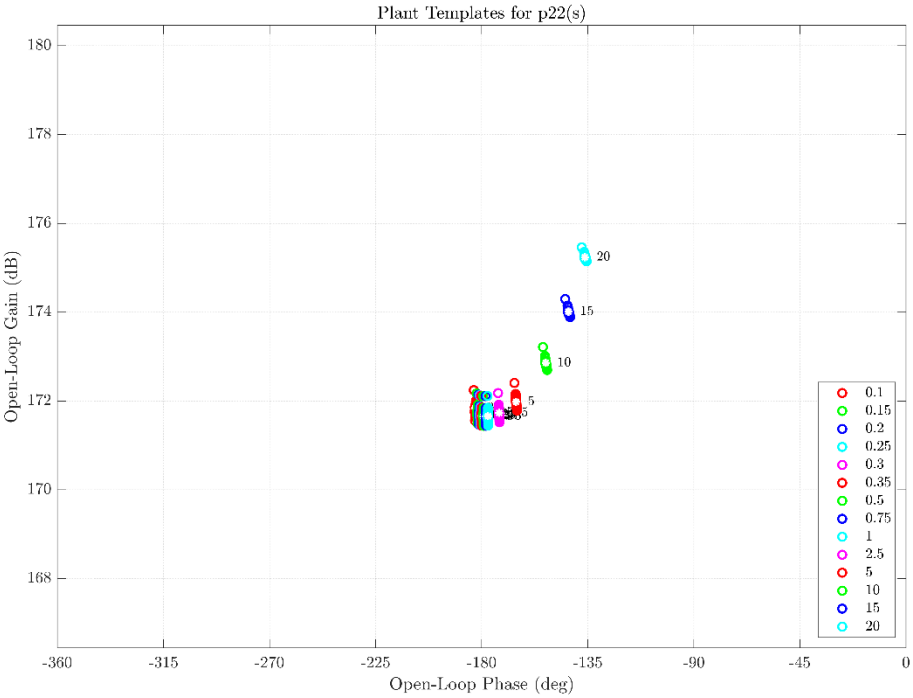

Figure 5: Plant template for P_{22}

In addition, the generated bounds and their intersections are presented below.

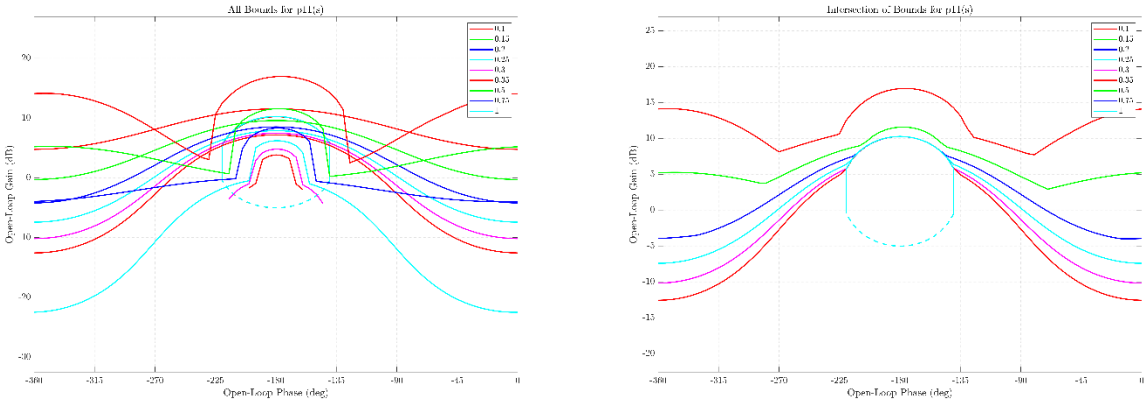

Figure 6: All bounds (left) and their intersection (right) for P_{11}

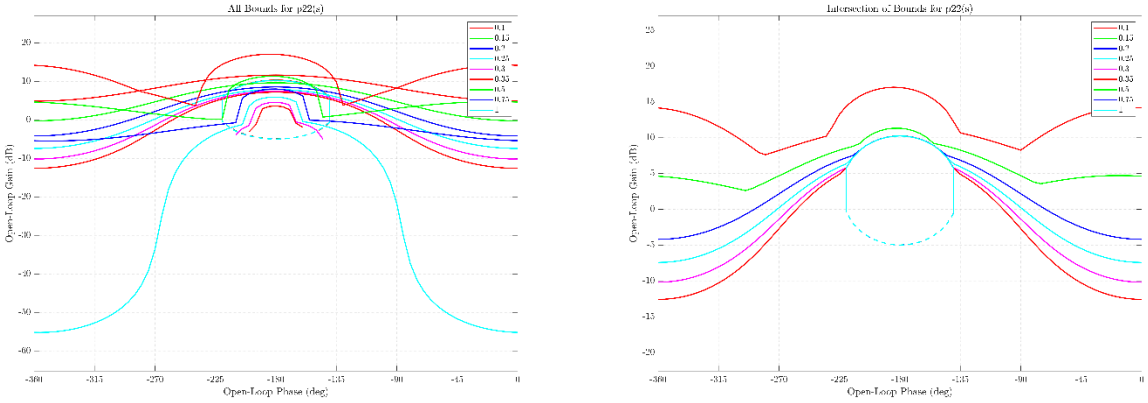

Figure 7:All bounds (left) and their intersection (right) for P_{22}

The designed controllers are presented below,

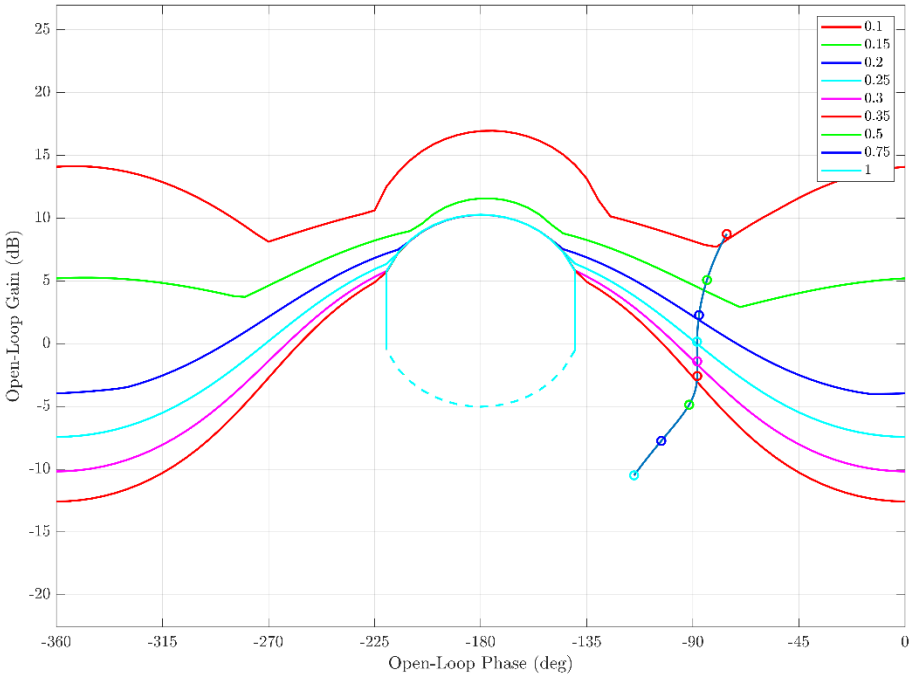

Figure 8: Loopshaping for $L_{0\_11} = P_{0\_11}G_{11}$

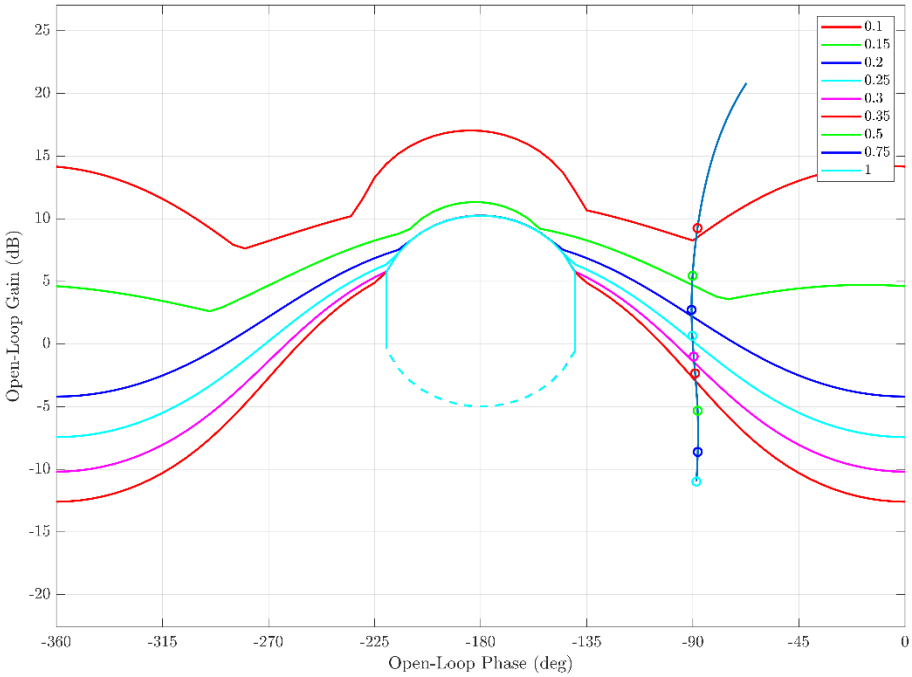

Figure 9: Loopshaping for $L_{0\_22} = P_{0\_22}G_{22}$

The results of the simulation are presented below,

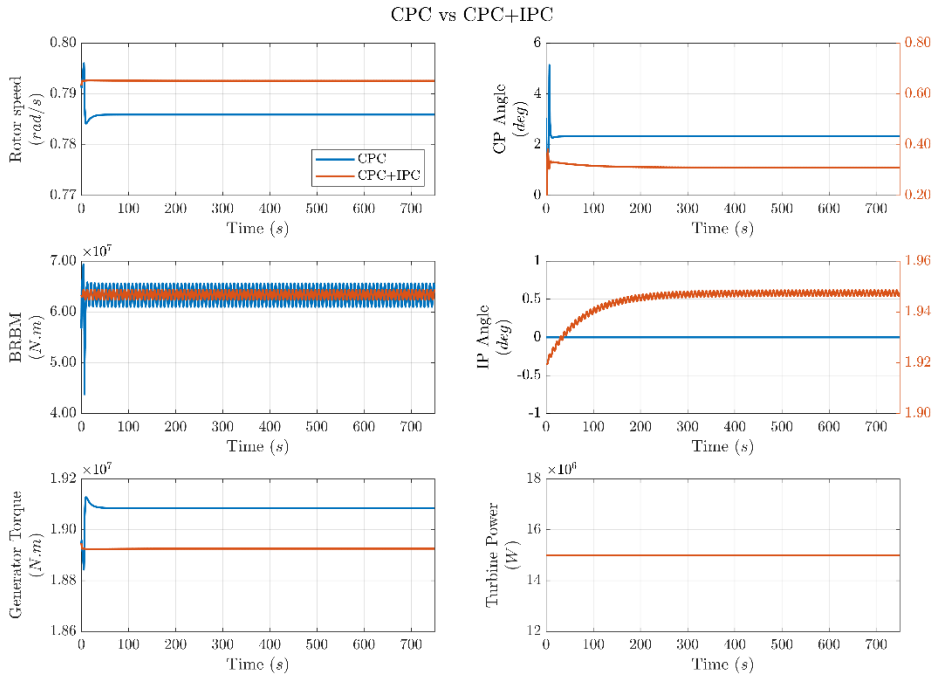

Figure 10: CPC vs CPC+IPC simulation results

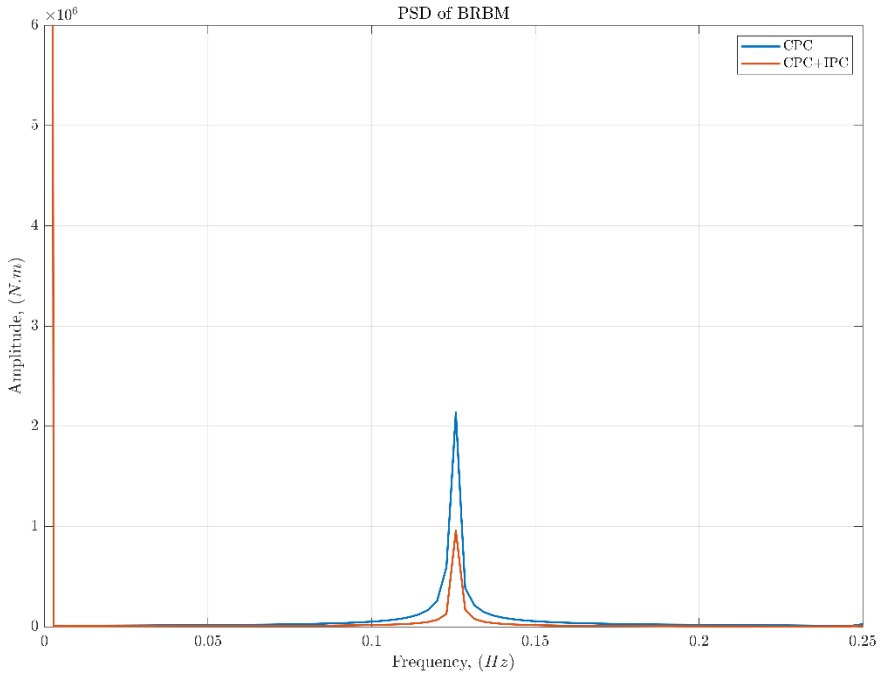

Figure 11: CPC vs CPC+IPC exhibits a 55% reduction in BRBM frequency amplitude

Stability and Performance Specifications

Stability Specification

$$\left|\frac{P(s)G(s)}{1+P(s)G(s)}\right| \le \delta_1(\omega) = W_s = 1.46, \qquad \omega \in \begin{bmatrix} 0.10, & 0.15, & 0.20, & 0.25, \\ 0.30, & 0.35, & 0.50, & 0.75, \\ & & 1.00 & \end{bmatrix}$$

Where Ws=1.46 corresponds to PM=40.05° and GM=4.53 dB.

Performance Specifications

1- Sensitivity (output disturbance rejection)

$$\left|\frac{1}{1+P(s)G(s)}\right| \le \delta_3(\omega) = \frac{1/a_d}{1/a_d + 1}, \qquad \omega \in \begin{bmatrix} 0.10, & 0.15, & 0.20, \\ 0.25, & 0.30, & 0.35 \end{bmatrix}$$

Where $a_d = 0.25$.

2- Reference tracking specification

$$\delta_{6\_lo}(\omega) \le \left|F(s)\frac{P(s)G(s)}{1+P(s)G(s)}\right| \le \delta_{6\_up}(\omega), \qquad \omega \in \begin{bmatrix} 0.10, & 0.15, & 0.20, \\ 0.25, & 0.30, & 0.35 \end{bmatrix}$$

with

$$\delta_6(\omega) = \frac{(1-\epsilon_{lo})}{\left(s/a_{lo}+1\right)^2}, \qquad \epsilon_{lo} \ge 0$$

and

$$\delta_6(\omega) = \frac{\left(s/a_{up}\right)\left(1+\epsilon_{up}\right)}{\left(s/\omega_n\right)^2 + 2\zeta/\omega_n\, s + 1}, \quad \epsilon_{up} \ge 0, \qquad \zeta = 0.8, \qquad \omega_n = \frac{1.25 a_{up}}{\zeta}$$

Where $a_{lo} = 0.75$, $\epsilon_{lo} = 0$ and $a_{up} = 1.00$, $\epsilon_{up} = 0$